AIP | Applied Physics Letters

Stoichiometry-driven metal-to-insulator transition in NdTiO3/SrTiO3 heterostructures

Peng Xu, Daniel Phelan, Jong Seok Jeong, K. Andre Mkhoyan, and Bharat Jalan

Citation: Applied Physics Letters **104**, 082109 (2014); doi: 10.1063/1.4866867
View online: http://dx.doi.org/10.1063/1.4866867
View Table of Contents: http://scitation.aip.org/content/aip/journal/apl/104/8?ver=pdfcov
Published by the AIP Publishing

Stoichiometry-driven metal-to-insulator transition in $NdTiO_3/SrTiO_3$ heterostructures

Peng Xu, Daniel Phelan, Jong Seok Jeong, K. Andre Mkhoyan, and Bharat Jalan[a)]
Department of Chemical Engineering and Materials Science, University of Minnesota, Minneapolis, Minnesota 55455, USA

(Received 22 January 2014; accepted 12 February 2014; published online 27 February 2014)

By controlling stoichiometry via a hybrid molecular beam epitaxy approach, we report on the study of thin film growth and the electronic transport properties of phase-pure, epitaxial $NdTiO_3/SrTiO_3$ heterostructures grown on (001) $(La_{0.3}Sr_{0.7})(Al_{0.65}Ta_{0.35})O_3$ (LSAT) substrates as a function of cation stoichiometry in $NdTiO_3$. Despite the symmetry mismatch between bulk $NdTiO_3$ and the substrate, $NdTiO_3$ films grew in an atomic layer-by-layer fashion over a range of cation stoichiometry; however amorphous films resulted in cases of extreme cation non-stoichiometry. Temperature-dependent sheet resistance measurements were consistent with Fermi-liquid metallic behavior over a wide temperature range, but revealed a remarkable crossover from metal-to-insulator (M-I) type behavior at low temperatures for all compositions. A direct correlation between cation stoichiometry, transport behavior, and the temperature of M-I transition is established. © *2014 AIP Publishing LLC*. [http://dx.doi.org/10.1063/1.4866867]

Complex oxides exhibit a range of electronic, magnetic and collective phenomena. One example includes metal-to-insulator transitions (MITs), which can be controlled by either electron correlations or disorder and are often referred to as Mott-Hubbard MITs or Anderson MITs, respectively.[1] However, one of the issues with their study in bulk materials is that these two effects often accompany one another. For instance, chemical or vacancy doping influences electron correlations, but also introduces disorder.[2] Thin films and heterostructures allow for independent control of these two effects via modulation doping, strain, and dimensionality. Examples of experimental attempts to separate out the effects of electron correlations and disorder include heterostructures involving cuprate oxides[3] (as well as a range of other magnetic oxides[4,5]), and interfaces between band and Mott insulators.[6–9] Nevertheless, even in such heterostructures, the disorder or defects present in one layer can still influence the electronic and magnetic properties of the interfaces.[10–15] Very recently, Warusawithana *et al.*[16] have shown via $LaAlO_3/SrTiO_3$ heterostructures grown by molecular beam epitaxy (MBE) that a small amount of cation non-stoichiometry of $LaAlO_3$ is vital for forming an interfacial electron gas.

In an attempt to investigate the role of cation stoichiometry on interfacial electronic transport at polar/nonpolar oxide interfaces, this Letter focuses on the hybrid MBE growth of $NdTiO_3/SrTiO_3$ heterostructures and their transport properties as a function of Ti/Nd cation ratio in the $NdTiO_3$ layers. $NdTiO_3/SrTiO_3$ is reminiscent of $LaAlO_3/SrTiO_3$ in that both bulk $LaAlO_3$ and $NdTiO_3$ are insulators with trivalent A-site lanthanides, and moreover, both interfaces share polar discontinuity. On the other hand, these two heterostructures differ by the fact that bulk $NdTiO_3$ contains two magnetic ions (Nd^{3+} and Ti^{3+}), which could lead to additional functionality; furthermore, the presence of a Ti^{3+} d^1 electron can further complicate the electronic properties. Bulk $NdTiO_3$ is an antiferromagnetic Mott-insulator with a Mott-Hubbard gap of 0.8 eV;[17] but dissimilar to $LaAlO_3$, cation non-stoichiometry, in particular, Nd deficiency, leads to an insulator-metal transition in the bulk, which occurs due to the interplay between disorder and the Coulomb interaction.[17] This interplay is further expected to play a significant role in determining the interfacial transport properties of the $NdTiO_3/SrTiO_3$ interface and could perhaps pave the way to novel phenomena in defect-managed heterostructures.

Bulk $NdTiO_3$ is an orthorhombic perovskite (space group *Pbnm*) with lattice parameters of $a_o = 5.525$ Å, $b_o = 5.659$ Å, and $c_o = 7.791$ Å.[18] Two corresponding pseudocubic lattice parameters, given by the d-spacings of the $(110)_o$ and $(002)_o$ Bragg reflections (subscript o refers to the orthorhombic setting), are $a_1^{pc} = d_{110o} = 3.953$ Å and $a_2^{pc} = d_{002o} = 3.896$ Å, respectively. $(La_{0.3}Sr_{0.7})(Al_{0.65}Ta_{0.35})O_3$ (LSAT) is a cubic perovskite with a lattice parameter of $a = 3.868$ Å, which yields compressive in-plane strains of −2.15% (on a_1^{pc}) and −1.43% (on a_2^{pc}) for $NdTiO_3$ on (001) LSAT. Corresponding out-of-plane lattice parameters are thus estimated to be 3.972 Å and 4.005 Å given in-plane strains on a_1^{pc} and a_2^{pc}, respectively, using the elastic tensor of $NdTiO_3$[19] and assuming that films are completely coherent to the substrate. We note that when $NdTiO_3$ is grown on LSAT, its symmetry is modified into a (pseudo) tetragonal one (subscript t) with $a_t = b_t < c_t$, where c_t is the out-of-plane lattice parameter, and that the film with the lowest in-plane strain will grow with an expected out-of-plane lattice parameter, $c_t = 4.005$ Å, which we have estimated above.

Phase-pure, epitaxial $NdTiO_3$ films were grown on (001) LSAT substrates (Crystec GmbH, Germany) using an oxide MBE system (EVO 50, Omicron Nanotechnology, Germany) with a base pressure of 10^{-10} Torr. Prior to the film growth, a ~500 nm thick Ta layer was sputter-deposited at room temperature on the back of the substrate to improve heat transfer between the film and the substrate heater. Substrates were

a)Email: bjalan@umn.edu

then sequentially cleaned in acetone, isopropanol, and methanol and were then baked at ~200 °C in the MBE load lock before being transferred into the growth chamber. $NdTiO_3$ films were grown using a hybrid MBE approach (traditionally known as metal-organic or organometallic MBE[20,21]), which employs a metal-organic precursor of titanium tetra-isopropoxide (TTIP) (99.999% from Sigma-Aldrich, USA) as a Ti source and an effusion cell for Nd (99.99% from Ames Lab, USA). No additional oxygen was used since TTIP also supplies oxygen. Growth conditions for cation stoichiometric $NdTiO_3$ were identified at the substrate temperature of 900 °C (thermocouple) by varying the TTIP/Nd flux ratio, where the TTIP flux was kept constant and the Nd flux was varied by changing effusion cell temperature between 960 °C and 1015 °C. To grow $NdTiO_3/SrTiO_3$ heterostructures, a ~ 3 nm thick coherently strained, stoichiometric $SrTiO_3$ buffer layer was grown prior to $NdTiO_3$ thin films, using the same approach as described elsewhere.[22] The growth mode, film thickness, and surface morphology were obtained using *in-situ* Reflection High-Energy Electron Diffraction (RHEED) (Staib Instruments) technique. Further structural characterizations were performed using *ex-situ* techniques including high-resolution x-ray diffraction using a Philips Panalytical X'Pert thin-film diffractometer with Cu K_α radiation, x-ray photoelectron spectroscopy (XPS), atomic force microscopy (AFM), and scanning transmission electron microscopy (STEM). XPS spectra were obtained with SSX-100 XPS system using a monochromatic Al K_α x-ray source operated at 200 W. The size of x-ray beam was ~1 × 1 mm^2 and the energy resolution of the instrument was 0.8 eV. The instrument was calibrated with reference to the Au $4f_{7/2}$ peak (84.00 eV) and the separation between Cu $2p_{3/2}$ and Cu3s peaks was set at 810.08 eV. Survey spectra were collected using 150 eV pass energy and high-resolution spectra were obtained using 50 eV pass energy, giving accuracy within 0.3 eV for peak position determination. Photoelectron energy drift due to charging effect was offset with reference to the adventitious C 1 s peak (284.6 eV). The relative element contents in $NdTiO_3$ film were calculated using the Nd $3d_{5/2}$ and Ti $2p_{3/2}$ peaks with relative sensitivity factor 19.33 and 4.69 given by Electron Spectroscopy for Chemical Analysis (ESCA) analysis software library. Coupled 2θ-ω scans and grazing incidence x-ray reflectivity (GIXR) measurements were used to determine the out-of-plane lattice parameter and film thickness (consistent with the thickness determined using RHEED oscillations), respectively. AFM in contact mode was used to determine the surface morphology. High-angle annular dark-field (HAADF) STEM images were obtained using an aberration-corrected monochromatic FEI Titan G2 60–300 operated at 300 kV. The semi-convergent angle of the incident beam was 21.4 mrad and HAADF images were obtained with a detector angle of 58.5–200 mrad. DC transport measurements were performed in a Physical Property Measurement System (Quantum Design PPMS) using van der Pauw geometry. 300 nm of Au on top of 50 nm of Ti were sputtered as contacts for the $NdTiO_3/SrTiO_3$ heterostructures, while 300 nm of Au on 20 nm Ni on top of 40 nm of Al were sputtered as contacts for $SrTiO_3$ films. It is noted that the film thicknesses in this study were kept constant at ~6 nm.

We begin by discussing growth of $NdTiO_3$ directly on (001) LSAT. Figure 1 shows an x-ray 2θ-ω scan of a 6 nm thick $NdTiO_3$ film, which is consistent with the growth of phase pure, epitaxial $NdTiO_3$ on the (001) LSAT substrate. The out-of-plane lattice parameter, c_t (used as a sensitive probe to stoichiometry and relaxation) measured using first order film reflection (3.99 ± 0.01 Å, see inset of Fig. 1(a)) was in excellent agreement with our calculated estimate of the out-of-plane lattice parameter (4.005 Å) indicating that the film was coherently strained and nearly stoichiometric. This film was obtained using a Ti/Nd flux ratio of 9.6. Identical values of c_t were obtained for the samples with a buffer $SrTiO_3$ layer, and as the Ti/Nd flux ratio was tuned away from this value (either direction), c_t was found to decrease.[23] We argue that the peak in c_t close to the theoretically calculated value corresponds to 1:1 Ti:Nd stoichiometry. Extreme deviations from this ratio led to the absence of film diffraction peaks, suggesting that they were amorphous. We note that the decrease in c_t is in sharp contrast to the behavior observed in many complex oxide systems where the out-of-plane lattice parameter often increases with non-stoichiometry defects.[24–26] Using transmission electron microscopy, we demonstrate below that strain relaxation does not occur for 6 nm thick stoichiometric films, but the trend of c_t decreasing with increasing non-stoichiometry observed in the present case could be due to a complex relationship between strain relaxation, non-stoichiometry, and c_t and thus should not be attributed only to non-stoichiometric defects. For instance, strain relaxation can cause a decrease in the out-of-plane lattice parameter, which has been shown to occur at much lower film thicknesses in complex oxide for non-stoichiometric compositions.[27]

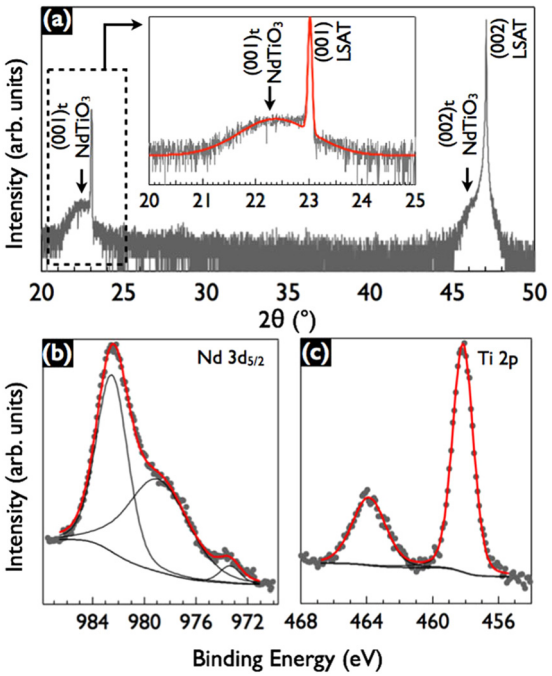

FIG. 1. (a) High-resolution x-ray 2θ-ω scan of 6 nm thick $NdTiO_3$ film grown on (001) LSAT substrate. The inset shows a magnified version of $NdTiO_3$ film reflection corresponding to $(001)_t$ $NdTiO_3$ (t refers to pseudo-tetragonal unit cell) on (001) LSAT substrate and is fitted using Gaussian. (b) and (c) Nd $3d_{5/2}$ and Ti 2p spectra for 6 nm thick $NdTiO_3$ film grown on (001) LSAT. $NdTiO_3$ film was grown using Ti/Nd flux ratio of 9.6.

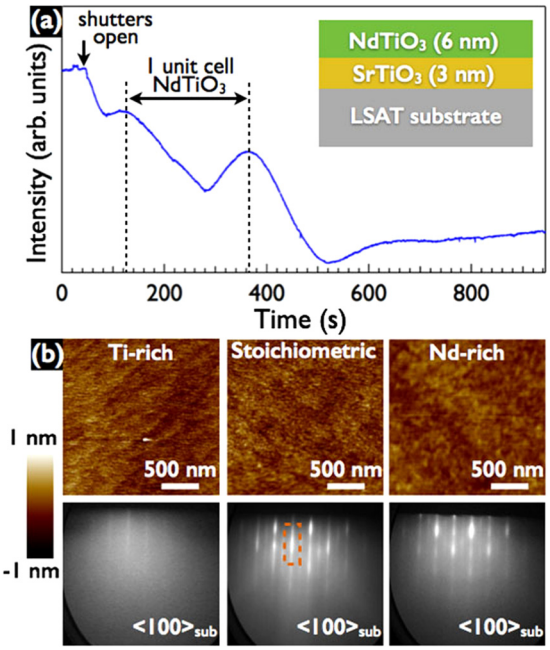

FIG. 2. (a) Time-dependent reflection high-energy electron diffraction intensity oscillations for stoichiometric $NdTiO_3$ film grown on LSAT with 3 nm thick $SrTiO_3$ buffer layer. (b) AFM image and the corresponding RHEED pattern after growth of $NdTiO_3$ films as a function of cation stoichiometry of $NdTiO_3$.

In order to further substantiate the cation stoichiometry, XPS measurements were performed on the same sample which we have argued above to possess 1:1 Ti:Nd stoichiometry. The XPS results confirmed 1:1.03 ratio for Ti:Nd (see Figs. 1(b) and 1(c)) for stoichiometric $NdTiO_3$. It is noted that while XPS may not be used as a standalone measure of film's stoichiometry, often due to surface effects, the results obtained here are consistent with the HRXRD data.

Figure 2(a) shows the time-dependent RHEED intensity oscillations followed by a nearly constant intensity after 600 s during the growth of the stoichiometric $NdTiO_3$ film. The fact that the intensity oscillations change to a nearly constant intensity indicates that film initially grew in a layer-by-layer fashion, before transitioning to a step-flow-growth mode. The result is consistent with the observed atomic terraces in the AFM images (Fig. 2(b)). Irrespective of the symmetry mismatch and the cation stoichiometry, $NdTiO_3$ films showed atomic terraces in AFM.[23] No such atomic terraces have been reported in similar heterostructure systems, such as $GdTiO_3/SrTiO_3$[28] and $LaAlO_3/SrTiO_3$.[29] We suggest that these may appear in the present case because of the less-distorted $NdTiO_3$ structure and the better lattice-matching of the $NdTiO_3/SrTiO_3$/LSAT systems. Spotty RHEED patterns were observed for both Ti- and Nd-rich films, which further disappeared for extremely non-stoichiometric compositions indicating amorphous morphology (Fig. 2(b)). To further obtain insight into the structure, atomic number-sensitive HAADF STEM image of $NdTiO_3/SrTiO_3$ heterostructures was taken (Fig. 3), which confirmed the epitaxial relationship, abrupt chemical interface, phase purity, and the absence of other extended defects.

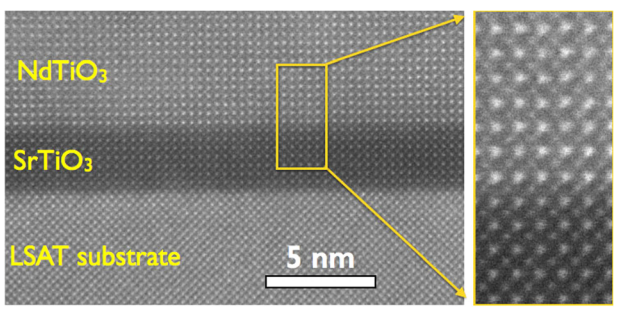

FIG. 3. Atomic-number sensitive HAADF STEM image of $NdTiO_3$ film grown on 3 nm thick $SrTiO_3$ buffer layer on LSAT substrate. The inset shows the magnified version of the interface enclosed in the box showing atomically abrupt interface.

We now turn to the transport properties of the films. No measurable conductivity was observed in an as-grown 3 nm $SrTiO_3$ film on a (001) LSAT substrate. However, stoichiometric $NdTiO_3$ films grown directly on LSAT substrates showed semiconducting behavior with a room temperature resistivity of 1.8 Ω cm and a temperature-dependence consistent with an Arrhenius law with an activation energy of 0.098 eV,[23] which is remarkably close to the value expected from the small polaron hopping conduction in nearly stoichiometric bulk $NdTiO_3$ (0.084 eV).[17] The higher value of resistivity obtained in our stoichiometric films as compared to that of bulk $NdTiO_3$ single crystals (~0.3 Ω cm) could be due to the better stoichiometry control or due to the reduction of *bandwidth* under compressive strain.

Figure 4(a) shows the temperature dependence of the sheet resistance (R_s) for $NdTiO_3/SrTiO_3$/LSAT heterostructures as a function of cation stoichiometry of $NdTiO_3$. The sample with the stoichiometric composition (i.e., with Ti/Nd flux ratio = 9.6) had the lowest R_s, n-type carriers with a sheet carrier density of $1.2 \times 10^{15}\,cm^{-2}$ and a mobility of

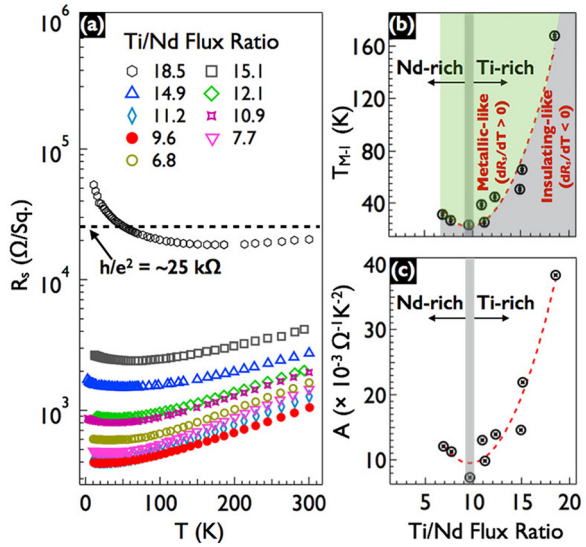

FIG. 4. (a) Sheet resistance (R_s) vs. temperature (T) as function of Ti/Nd flux ratio indicating the metal-to-insulator behavior at low temperature. Dashed line represents the Mott minimum metallic conductivity (e^2/h, $\sim 25\,k\Omega^{-1}$). (b) Crossover temperature between metal-to-insulator behavior, $T_{M\text{-}I}$ illustrating the metallic-to-insulating like behavior as a function of Ti/Nd flux ratio. (c) Value of coefficient A as a function of Ti/Nd flux ratio. The dashed lines show quadratic fits to the data. Vertical line corresponds to the stoichiometric composition.

$\sim 6\,cm^2\ V^{-1}\ s^{-1}$ at room temperature. Upon increasing non-stoichiometry, the room temperature R_s was found to increase, approaching a metal-to-insulator transition near the Mott minimum metallic conductivity (e^2/h, $\sim 25\,k\Omega^{-1}$).[30] Moreover, regardless of the cation stoichiometry, all samples in the metallic regime showed n-type carriers with remarkably high sheet carrier densities of $2 \times 10^{14}\,cm^{-2}$–$1.2 \times 10^{15}\,cm^{-2}$ and mobilities of 2–6 $cm^2\ V^{-1}\ s^{-1}$ at room temperature.[23] The origin of the high electron density (exceeding $^1/_2$ electron/unit cell, as one would expect from the electronic reconstruction model using similar material systems[31,32]) is surprising and may indicate that an additional mechanism(s) is at play. It is however evident that conduction is associated with the interface given that individual layers of $NdTiO_3$ and $SrTiO_3$, when grown separately on LSAT substrates, show semiconducting or insulating behavior as discussed earlier. Moreover, it was found that the temperature coefficient of sheet resistance (dR_s/dT) changes in sign from positive to negative at low temperature, with a minimum in resistance occurring at a finite temperature for all samples. Similar behavior has been reported in the literature for related heterostructures and has been attributed to weak localization.[32,33] In the metallic regime ($dR_s/dT > 0$), R_s was analyzed using the Fermi-liquid model:

$$R_S = R_0 + AT^2,$$

where R_0 is the residual sheet resistance due to impurity scattering, A is a constant, which represents extent of correlation strength (driven by electron-electron interaction or disorder) in the metallic state, and T is the temperature. The T^2 dependence of R_s in the metallic regime implicates the electron-electron interaction as the dominant scattering mechanism up to room temperature. Remarkably, it was found that the crossover temperature, $T_{M\text{-}I}$, of the metal-to-insulator behavior and the value of the coefficient A as determined from the fitting, were strongly correlated with the cation stoichiometry of $NdTiO_3$ (Figs. 4(b) and 4(c)). Regardless of whether $NdTiO_3$ films in the heterostructures were Nd- or Ti-rich, the value of $T_{M\text{-}I}$ and coefficient A increased, indicating these values were minimized for the stoichiometric composition. Furthermore, a sharp increase in the value of A near the metal-to-insulator transition (as a function of Ti/Nd ratio) suggests that strong electron mass enhancement is driven by disorder, introduced by non-stoichiometry. Future experiments and theory will be directed to address the origin of the high carrier density at these interfaces and the contribution of the Coulomb interaction to the metal-to-insulator transition, which is always present.

In summary, epitaxial, phase pure, and stoichiometric $NdTiO_3$ films have been grown in an atomic layer-by-layer fashion using the hybrid MBE approach with excellent control over cation stoichiometry. Irrespective of cation stoichiometry, transport measurement of $NdTiO_3/SrTiO_3$/LSAT heterostructures yielded remarkably high room-temperature carrier density and an upturn in R_s at low temperature. A strong correlation between cation stoichiometry, $T_{M\text{-}I}$, and the coefficient A was observed. We suggest that the fact that both $T_{M\text{-}I}$ and A increase for both Nd- and Ti-rich films can be used as a probe of cation stoichiometry. We further argue that the ability to control MIT using stoichiometry control can have serious implications for device development. For instance, stoichiometry control can be first employed to bring the sample near the MIT transition, where carrier control via electrostatic gating can further be used to drive the transition.

The authors thank Professor Mike Manno and Professor Chris Leighton for helpful discussion and Dr. Bing Luo for XPS analysis. This work was partially supported from the Office of the Vice President for Research, University of Minnesota and by the National Science Foundation through the University of Minnesota MRSEC under award number DMR-0819885. We also acknowledge use of facilities at the UMN Characterization Facility and the Nanofabrication Center.

[1]M. Imada, A. Fujimori, and Y. Tokura, Rev. Mod. Phys. **70**, 1039 (1998).
[2]J. B. Goodenough, Localized to Itinerant Electronic Transition in Perovskites Oxides, in *Structure and Bonding* (Springer-Verlag, New York, 1998).
[3]M. Nakamura, A. Sawa, H. Sato, H. Akoh, M. Kawasaki, and Y. Tokura, Phys. Rev. B **75**, 155103 (2007).
[4]C. H. Ahn, J. M. Triscone, and J. Mannhart, Nature **424**, 1015 (2003).
[5]S. Yunoki, A. Moreo, E. Dagotto, S. Okamoto, S. S. Kancharla, and A. Fujimori, Phys. Rev. B **76**, 064532 (2007).
[6]R. Scherwitzl, P. Zubko, I. G. Lezama, S. Ono, A. F. Morpurgo, G. Catalan, and J. M. Triscone, Adv. Mater. **22**, 5517 (2010).
[7]T. A. Cain, P. Moetakef, C. A. Jackson, and S. Stemmer, Appl. Phys. Lett. **101**, 111604 (2012).
[8]M. Hosoda, C. Bell, Y. Hikita, and H. Y. Hwang, Appl. Phys. Lett. **102**, 091601 (2013).
[9]J. Son, B. Jalan, A. P. Kajdos, L. Balents, S. J. Allen, and S. Stemmer, Appl. Phys. Lett. **99**, 192107 (2011).
[10]H. W. Jang, D. A. Felker, C. W. Bark, Y. Wang, M. K. Niranjan, C. T. Nelson, Y. Zhang, D. Su, C. M. Folkman, S. H. Baek, S. Lee, K. Janicka, Y. Zhu, X. Q. Pan, D. D. Fong, E. Y. Tsymbal, M. S. Rzchowski, and C. B. Eom, Science **331**, 886 (2011).
[11]T. Higuchi, Y. Hotta, T. Susaki, A. Fujimori, and H. Y. Hwang, Phys. Rev. B **79**, 075415 (2009).
[12]B. A. Gray, E. J. Moon, I. C. Tung, M. Kareev, J. Liu, D. J. Meyers, M. J. Bedzyk, J. W. Freeland, and J. Chakhalian, "Enhanced spin and electronic reconstructions at the cuprate-manganite interface," preprint arXiv:1301.3736v1 [cond-mat.str-el] (2013).
[13]Z. Wang, M. Okude, M. Saito, S. Tsukimoto, A. Ohtomo, M. Tsukada, M. Kawasaki, and Y. Ikuhara, Nat. Commun. **1**, 106 (2010).
[14]L. Qiao, T. C. Droubay, T. Varga, M. E. Bowden, V. Shutthanandan, Z. Zhu, T. C. Kaspar, and S. A. Chambers, Phys. Rev. B **83**, 085408 (2011).
[15]H. K. Sato, C. Bell, Y. Hikita, and H. Y. Hwang, Appl. Phys. Lett. **102**, 251602 (2013).
[16]M. P. Warusawithana, C. Richter, J. A. Mundy, P. Roy, J. Ludwig, S. Paetel, T. Heeg, A. A. Pawlicki, L. F. Kourkoutis, M. Zheng, M. Lee, B. Mulcahy, W. Zander, Y. Zhu, J. Schubert, J. N. Eckstein, D. A. Muller, C. S. Hellberg, J. Mannhart, and D. G. Schlom, Nat. Commun. **4**, 2351 (2013).
[17]A. S. Sefat, J. E. Greedan, G. M. Luke, and M. Niewczas, Phys. Rev. B **74**, 104419 (2006).
[18]A. C. Komarek, H. Roth, M. Cwik, W. D. Stein, J. Baier, M. Kriener, F. Bouree, T. Lorenz, and M. Braden, Phys. Rev. B **75**, 224402 (2007).
[19]B. Steele, A. D. Burns, A. Chernatynskiy, R. W. Grimes, and S. R. Phillpot, J. Mater. Sci. **45**, 168 (2010).
[20]L. King, K. Y. Hsieh, D. J. Lichtenwalner, and A. I. Kingon, Appl. Phys. Lett. **59**, 3045 (1991).
[21]K. Endo, S. Saya, S. Misawa, and S. Yoshida, Thin Solid Films **206**, 143 (1991).
[22]T. Wang, K. Ganguly, P. Marshal, P. Xu, and B. Jalan, Appl. Phys. Lett. **103**, 212904 (2013).
[23]See supplementary material at http://dx.doi.org/10.1063/1.4866867 for further information about the film resistivity, surface morphology and

stoichiometry-dependent out-of-plane lattice parameter, electron concentration, and mobility.
[24]C. M. Brooks, L. F. Kourkoutis, T. Heeg, J. Schubert, D. A. Muller, and D. G. Schlom, Appl. Phys. Lett. **94**, 162905 (2009).
[25]B. Jalan, R. Engel-Herbert, N. J. Wright, and S. Stemmer, J. Vac. Sci. Technol. A **27**, 461 (2009).
[26]T. Ohnishi, K. Shibuya, T. Yamamoto, and M. Lippmaa, J. Appl. Phys. **103**, 103703 (2008).
[27]E. Breckenfeld, A. B. Shah, and L. W. Martin, J. Mater. Chem. C **1**, 8052 (2013).
[28]P. Moetakef, J. Y. Zhang, S. Raghavan, A. P. Kajdos, and S. Stemmer, J. Vac. Sci. Technol. A **31**, 041503 (2013).
[29]D. L. Proffit, H. W. Jang, S. Lee, C. T. Nelson, X. Q. Pan, M. S. Rzchowski, and C. B. Eom, Appl. Phys. Lett. **93**, 111912 (2008).
[30]P. B. Chakraborty, K. Byczuk, and D. Vollhardt, Phys. Rev. B **84**, 035121 (2011).
[31]P. Moetakef, T. A. Cain, D. G. Ouellette, J. Y. Zhang, D. O. Klenov, A. Janotti, C. G. Van de Walle, S. Rajan, S. J. Allen, and S. Stemmer, Appl. Phys. Lett. **99**, 232116 (2011).
[32]J. Biscaras, N. Bergeal, A. Kushwaha, T. Wolf, A. Rastogi, R. C. Budhani, and J. Lesueur, Nat. Commun. **1**, 89 (2010).
[33]P. Moetakef, J. Y. Zhang, A. Kozhanov, B. Jalan, R. Seshadri, S. J. Allen, and S. Stemmer, Appl. Phys. Lett. **98**, 112110 (2011).